ORIGINAL ARTICLE

Cancer Science WILEY

VEGFR2 blockade augments the effects of tyrosine kinase inhibitors by inhibiting angiogenesis and oncogenic signaling in oncogene-driven non-small-cell lung cancers

Hiromi Watanabe[1] | Eiki Ichihara[2] | Hiroe Kayatani[1] | Go Makimoto[1] | Kiichiro Ninomiya[1] | Kazuya Nishii[1] | Hisao Higo[1] | Chihiro Ando[1] | Sachi Okawa[1] | Takamasa Nakasuka[1] | Hirohisa Kano[1] | Naofumi Hara[1] | Atsuko Hirabae[1] | Yuka Kato[3] | Takashi Ninomiya[1] | Toshio Kubo[4] | Kammei Rai[2] | Kadoaki Ohashi[2] | Katsuyuki Hotta[3] | Masahiro Tabata[4] | Yoshinobu Maeda[1] | Katsuyuki Kiura[2]

[1]Department of Hematology, Oncology and Respiratory Medicine, Okayama University Graduate School of Medicine, Dentistry, and Pharmaceutical Sciences, Okayama, Japan

[2]Department of Allergy and Respiratory Medicine, Okayama University Hospital, Okayama, Japan

[3]Center for Innovative Clinical Medicine, Okayama University Hospital, Okayama, Japan

[4]Center for Clinical Oncology, Okayama University Hospital, Okayama, Japan

Correspondence
Eiki Ichihara, Okayama University Hospital, 2-5-1 Shikata-cho Kita-ku, Okayama City, Okayama 700-8558, Japan.
Email: ichiha-e@md.okayama-u.ac.jp

Abstract

Molecular agents targeting the epidermal growth factor receptor (*EGFR*)-, anaplastic lymphoma kinase (*ALK*)- or c-*ros* oncogene 1 (*ROS1*) alterations have revolutionized the treatment of oncogene-driven non-small-cell lung cancer (NSCLC). However, the emergence of acquired resistance remains a significant challenge, limiting the wider clinical success of these molecular targeted therapies. In this study, we investigated the efficacy of various molecular targeted agents, including erlotinib, alectinib, and crizotinib, combined with anti-vascular endothelial growth factor receptor (VEGFR) 2 therapy. The combination of VEGFR2 blockade with molecular targeted agents enhanced the anti-tumor effects of these agents in xenograft mouse models of *EGFR*-, *ALK*-, or *ROS1*-altered NSCLC. The numbers of CD31-positive blood vessels were significantly lower in the tumors of mice treated with an anti-VEGFR2 antibody combined with molecular targeted agents compared with in those of mice treated with molecular targeted agents alone, implying the antiangiogenic effects of VEGFR2 blockade. Additionally, the combination therapies exerted more potent antiproliferative effects in vitro in *EGFR*-, *ALK*-, or *ROS1*-altered NSCLC cells, implying that VEGFR2 inhibition also has direct anti-tumor effects on cancer cells. Furthermore, VEGFR2 expression was induced following exposure to molecular targeted agents, implying the importance of VEGFR2 signaling in NSCLC patients undergoing molecular targeted therapy. In conclusion, VEGFR2 inhibition enhanced the anti-tumor effects of molecular targeted agents in various oncogene-driven NSCLC models, not only by inhibiting tumor angiogenesis but also by exerting direct antiproliferative effects on cancer cells. Hence, combination therapy with anti-VEGFR2 antibodies and molecular targeted agents could serve as a promising treatment strategy for oncogene-driven NSCLC.

1 | INTRODUCTION

The identification of oncogenic gene alterations has revolutionized the treatment of advanced non-small-cell lung cancer (NSCLC). Mutations in epidermal growth factor receptor (*EGFR*),[1] anaplastic lymphoma kinase (*ALK*),[2] and *c-ros* oncogene 1 (*ROS1*) genes[3] are among the most common oncogenic alterations in NSCLC,[4] and agents targeting these mutated proteins have been shown to exert strong anti-tumor effects.[5-7] However, a significant percentage of patients develop acquired resistance to these agents, hence the development of combination therapies is of high clinical importance.

Antiangiogenic agents suppress tumor growth by inhibiting the formation of new blood vessels.[8] The vascular endothelial growth factor (VEGF)-targeting antibody bevacizumab has been proven effective in combination with cytotoxic chemotherapy in patients with advanced NSCLC.[9] Moreover, the combination of bevacizumab with EGFR tyrosine kinase inhibitors (TKIs) exerted strong anti-tumor effects in *EGFR*-mutant NSCLC.[10] Notably, patients treated with the EGFR-TKI erlotinib plus bevacizumab had a median progression-free survival of 16.9 mo, compared with 13.3 mo in patients treated with erlotinib alone.[10] Similarly, combination of the anti-VEGFR2 antibody ramucirumab with erlotinib significantly prolonged the progression-free survival of patients with *EGFR*-mutant NSCLC compared with erlotinib alone (19.4 vs. 12.4 mo, $P < .0001$).[11] Although these data imply that targeting the VEGF pathway augments the anti-tumor effects of EGFR TKIs, the underlying mechanisms remain unclear. Furthermore, whether the combination of anti-VEGFR2 therapy with other targeted molecular therapies provides a clinical benefit in patients with oncogene-driven NSCLC remains to be elucidated.

In this study, we investigated the therapeutic effects of anti-VEGFR2 therapy in combination with different molecular targeted agents in oncogene-driven NSCLC, as well as explored the mechanisms underlying the synergistic effects of these therapies.

2 | MATERIALS AND METHODS

2.1 | Cell lines and reagents

PC-9 cells (EGFR Ex19 del E746_A750) were purchased from the European Collection of Authenticated Cell Cultures and A549 cells from the American Type Culture Collection. H3255 cells were kindly gifted by N Fujimoto and JM Kurie (MD Anderson Cancer Center, Houston, TX, USA). H3122 (*EML4-ALK* fusion) and HCC78 (*SLC34A2-ROS1* fusion) cells were kindly provided by William Pao (Vanderbilt University, Nashville, TN, USA). ABC-11 (*EML4-ALK* fusion) and ABC-20 (*CD74-ROS1* fusion) cells were established from NSCLC patients in our laboratory.[12,13] All cell lines were cultured in RPMI-1640 medium (Sigma-Aldrich) supplemented with 10% heat-inactivated fetal bovine serum and 1% penicillin/streptomycin; cells were maintained at 37°C in a 5% CO_2 humified atmosphere.

Ramucirumab and the anti-mouse VEGFR2 antibody DC101 were obtained from Eli Lilly. Erlotinib, osimertinib, alectinib, and crizotinib were purchased from Selleck Chemicals. All compounds were dissolved in dimethyl sulfoxide for in vitro studies.

Growth inhibition was measured using the modified 3-(4,5-dimethylthiazol-2-yl)-2,5-diphenyltetrazolium bromide (MTT) assay. Briefly, cells were seeded into 96-well plates at densities of 1000-8000 cells/well (PC-9:1000 cells/well; H3255/ABC-11/H3122: 3000 cells/well; HCC78: 2000 cells/well; ABC-20:8000 cells/well) and treated with each drug for 96 h.

2.2 | Antibodies, immunoblotting, and receptor tyrosine kinase array

The following antibodies were obtained from Cell Signaling Technology: phospho-EGFR (Tyr1068), EGFR, phospho-ALK (Tyr1282/1283), ALK, phospho-ROS1 (Tyr2274), ROS1, phospho-ERK1/2 (Thr202/Tyr204), ERK1/2, phospho-AKT (Ser473), AKT, GAPDH, and horseradish peroxidase-conjugated anti-rabbit IgG antibody.

For immunoblotting, cells were harvested, washed in phosphate-buffered saline, and lysed in radioimmunoprecipitation assay buffer (1% Triton X-100, 0.1% sodium dodecyl sulfate, 50 mmol/L Tris-HCl, pH 7.4, 150 mmol/L NaCl, 1 mmol/L EDTA, 1 mmol/L EGTA, 10 mmol/L β-glycerol-phosphate, 10 mmol/L NaF, and 1 mmol/L sodium orthovanadate) containing a protease inhibitor cocktail (Roche Applied Sciences). Proteins were separated by sodium dodecyl sulfate–polyacrylamide gel electrophoresis and then transferred onto membranes, which were then incubated with the indicated primary and secondary antibodies. Chemiluminescence was detected using an enhanced chemiluminescence plus reagent (GE Healthcare Biosciences).

Phospho-receptor tyrosine kinase arrays were performed using a phospho-receptor tyrosine kinase array kit (R&D Systems) in accordance with the manufacturer's instructions. Bands and dots were detected using the ImageQuant LAS-4000 imager (GE Healthcare Biosciences).

2.3 | Immunohistochemistry

Formalin-fixed, paraffin-embedded tissue blocks were cut into 5-μm-thick sections, placed on glass slides, and deparaffinized with D-limonene and graded alcohols. Antigen retrieval was performed by incubating the sections in 10 mmol/L sodium citrate buffer (pH 6.0) for 10 min at 95°C. Subsequently, the sections were incubated for 10 min in methanol containing 3% hydrogen peroxide to block endogenous peroxidase activity. After washing with Tris-buffered saline containing 0.1% Tween 20, tissues were incubated with normal goat serum for 60 min. Sections were probed with an anti-CD31 antibody (#77699; Cell Signaling Technology) and anti-VEGFR2 antibody(#2479S; Cell Signaling Technology) overnight at 4°C. Thereafter, the sections were incubated for 30 min with biotinylated anti-rabbit antibodies and avidin-biotinylated horseradish peroxidase conjugate (SignalStain

Boost IHC Detection Reagent #8114; Cell Signaling Technology). Finally, sections were incubated with 3,3-diaminobenzidine and counterstained with hematoxylin. The antibody dilutions were performed in accordance with the manufacturer's instructions.

2.4 | Quantitative reverse-transcription polymerase chain reaction (qRT-PCR)

RNA was extracted from cells using the RNeasy Mini Kit (Qiagen) in accordance with the manufacturer's instructions. *VEGFR2* copy number gain was assessed by qRT-PCR using the TaqMan probes and primers detailed in Table S1. PCR was run on the LightCycler Real-Time PCR System (Roche Applied Science), and gene dosage was calculated using a standard curve. The *VEGFR2/GAPDH* copy number ratio was also calculated.

2.5 | Small interfering RNA (siRNA) transfection

Transfection conditions for siRNA-mediated gene knockdown were optimized using *VEGFR2* siRNAs (Dharmacon Inc) and Lipofectamine Transfection Reagent (Thermo Fisher Scientific) in a 96-well plate format (PC-9:1500 cells/well; H3122: 3000 cells/well; ABC-20:8000 cells/well). Two predesigned gene-specific siRNAs were tested for each candidate gene, along with negative and positive controls (Dharmacon *VEGFR2* siRNA). Gene silencing efficiency was evaluated 48 h post-transfection by qRT-PCR.

2.6 | ELISA

Cells were seeded into 3.5 cm cell culture dishes (3.0×10^5 cells/dish), and the cell supernatant was collected after 24 h. The levels of VEGF-A were determined by Human VEGF Quantikine ELISA (R&D Systems) in accordance with the manufacturer's instructions.

2.7 | Xenograft mouse models

Female BALB/c nu/nu mice (6 wk old) were purchased from Charles River Laboratories). All mice were provided sterilized food and water and housed in a barrier facility under a 12-h light/dark cycle. Cancer cells ($2\text{-}5 \times 10^6$) were injected subcutaneously into the back on both sides of the mice. When the average tumor volume reached ~200 mm^3, the mice were randomly allocated into 4 treatment groups (4 mice/group): vehicle, DC101 (10 mg/kg/d), molecular targeted agent (erlotinib [30 mg/kg/d], osimertinib [5 mg/kg/d], alectinib [10 mg/kg/d], or crizotinib [50 mg/kg/d]), and DC101 combined with the molecular targeted agents. Vehicle and molecular targeted agents were administered by gavage once daily, 5 times weekly. DC101 was administered by intraperitoneal administration once daily, twice weekly.

Tumor volume (width^2 × length/2) was determined periodically. Statistical analyses were conducted using the tumor volumes measured on day 28. All experiments involving animals were performed under the auspices of the Institutional Animal Care and Research Advisory Committee at the Department of Animal Resources, Okayama University Advanced Science Research. The experiments were performed under the Policy on the Care and Use of the Laboratory Animals, Okayama University, and Fundamental Guidelines for Proper Conduct of Animal Experiment and Related Activities in Academic Research Institutions, Ministry of Education, Culture, Sports, Science and Technology of Japan. The experimental protocol was approved by the Animal Care and Use Committee of the Okayama University, Okayama, Japan (OKU-2018455).

2.8 | Statistical analysis

Statistical analysis was performed using STATA software (version 15; StataCorp). Differences between groups were compared using two-tailed paired Student *t* tests. *P*-values < .05 were considered statistically significant.

3 | RESULTS

3.1 | Anti-VEGFR2 therapy augments the efficacy of molecular targeted therapy in oncogene-driven cancer

Here, we investigated the effects of the anti-mouse VEGFR2 antibody DC101 on the efficacy of molecular targeted therapies in NSCLC harboring *EGFR*, *ALK*, or *ROS1* alterations. To this end, we used the *EGFR*-mutant PC-9 and H3255 cells, the *ALK*-rearranged H3122 and ABC-11 cells, and the *ROS1*-rearranged ABC-20 cells. We first assessed the efficacy of DC101 on erlotinib in PC-9 xenograft tumors, which harbor an *EGFR* exon 19 deletion. DC101 and erlotinib combination therapy exerted more potent anti-tumor effects compared with erlotinib monotherapy (Figure 1A). We also assessed the combination therapy in H3255 xenograft tumors harboring the *EGFR* exon 21 L858R point mutation. Both erlotinib monotherapy and the combination of DC101 with erlotinib almost completely inhibited tumor growth up to 60 d of treatment. Tumor regrowth was observed in the erlotinib monotherapy group after cessation of the treatment, whereas more durable tumor inhibition was observed in the combination therapy group (Figure 1B).

The efficacy of the combination of DC101 with EGFR TKIs was also investigated using osimertinib, a third-generation EGFR-TKI. The combination therapy provided significantly stronger anti-tumor effects in PC-9 xenograft tumors compared with osimertinib alone (Figure S1A). Similarly, the combination of DC101 with the ALK-TKI alectinib exerted stronger anti-tumor effects in *ALK*-rearranged H3122 tumors compared with alectinib monotherapy (Figure 1C). Similar results were obtained with *ALK*-rearranged
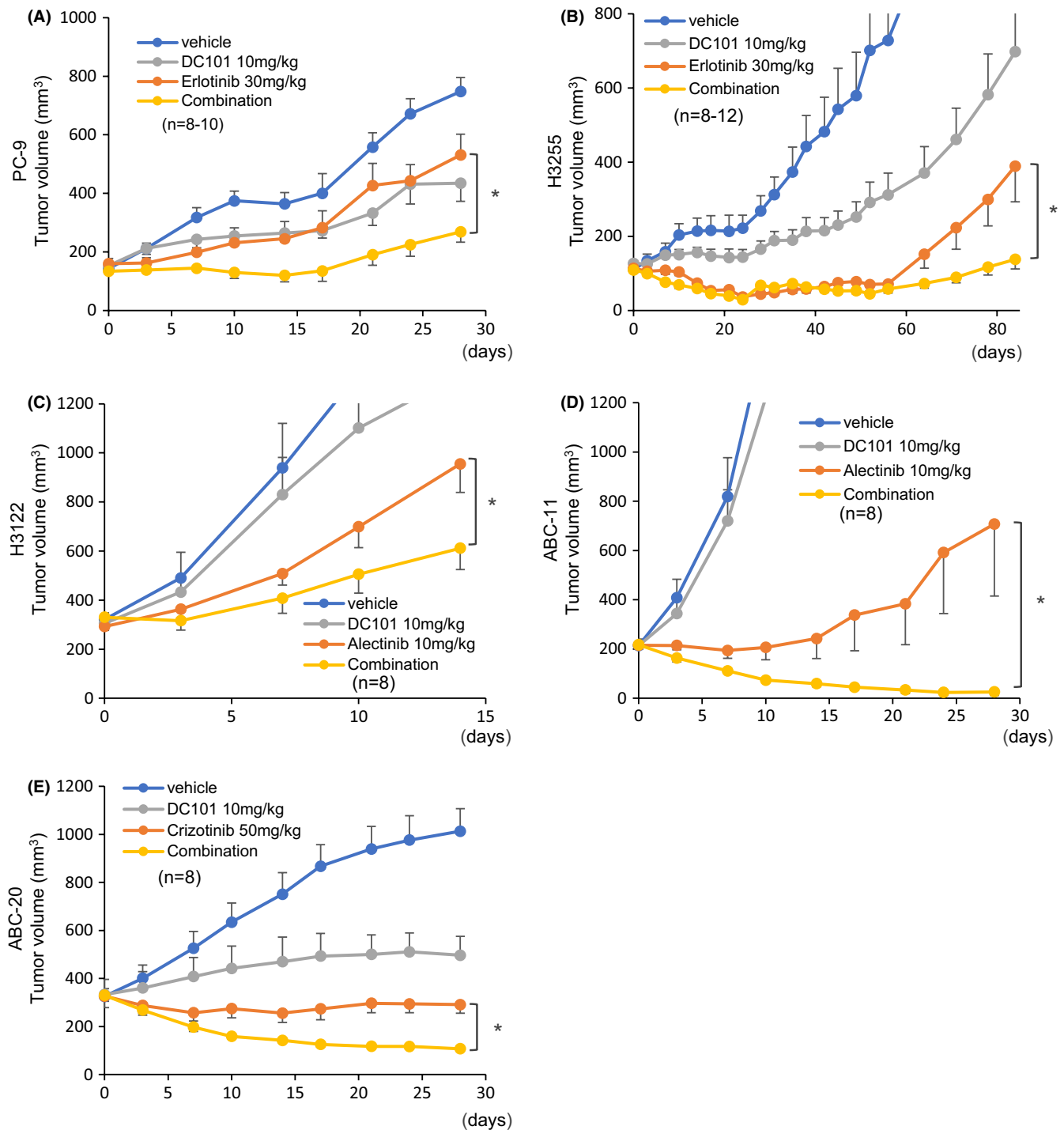
FIGURE 1 Combination of molecular targeted agents and VEGFR2 blockade in xenograft mouse models. Mice were transplanted with PC-9, H3255, H3122, ABC-11, or ABC-20 cells. Molecular targeted agents were orally administered 5 times weekly. DC101 was administered intraperitoneally (10 mg/kg/d) twice weekly. A, B, Mice bearing PC-9 or H3255 tumors were treated with vehicle, erlotinib (30 mg/kg/d), DC101, or erlotinib plus DC101 combination. In H3255-transplanted mice, the erlotinib dose was reduced to 15 mg/kg/d from day 21, and the treatment was discontinued from day 53. C, D, Mice bearing H3122 and ABC-11 tumors were treated with vehicle, alectinib (10 mg/kg/d), DC101, or alectinib plus DC101 combination. E, Mice bearing ABC-20 tumors were treated with vehicle, crizotinib (50 mg/kg/d), DC101, or crizotinib plus DC101 combination. Error bars represent standard errors; $*P < .05$

ABC-11 xenograft models, in which treatment with DC101 augmented the therapeutic effects of alectinib (Figure 1D). We also investigated the therapeutic effects of DC101 in *ROS1*-rearranged NSCLC using ABC-20 cells (*CD74-ROS1* fusion). DC101

significantly enhanced the anti-tumor effects of the ROS1-TKI crizotinib in ABC-20 tumors (Figure 1E). Notably, no significant toxicities were observed in mice treated with any of the combination therapies (Figures S1B and S2). *ROS1*-rearranged HCC78

cells failed to engraft even in highly immunosuppressed NOG mice (data not shown).

3.2 | Combination of anti-VEGFR2 antibody with molecular targeted therapy inhibits tumor angiogenesis

To elucidate the mechanisms underlying the enhanced anti-tumor effects of the combination of DC101 with molecular targeted therapy, we analyzed the extent of tumor angiogenesis in xenograft tumors. Anti-mouse CD-31 antibody stained the vessels, but anti-human CD-31 antibody did not (data not shown), suggesting that the tumor vessels were derived from mouse tissues. Anti-mouse CD31 immunostaining revealed that DC101 monotherapy or the combination of DC101 with erlotinib, alectinib, or crizotinib impaired angiogenesis in PC-9 (*EGFR*-mutant), H3122 (*ALK*-rearranged), and ABC-20 (*ROS1*-rearranged) xenograft tumors, respectively (Figures 2A and S1C). The combination treatments provided more profound antiangiogenic effects compared with the molecular targeted agents alone (Figures 2B,C and S1D), although quantification could not be

performed in PC-9 tumors due to their small size. These data imply that DC101 enhanced the anti-tumor effects of molecular targeted agents by inhibiting tumor angiogenesis.
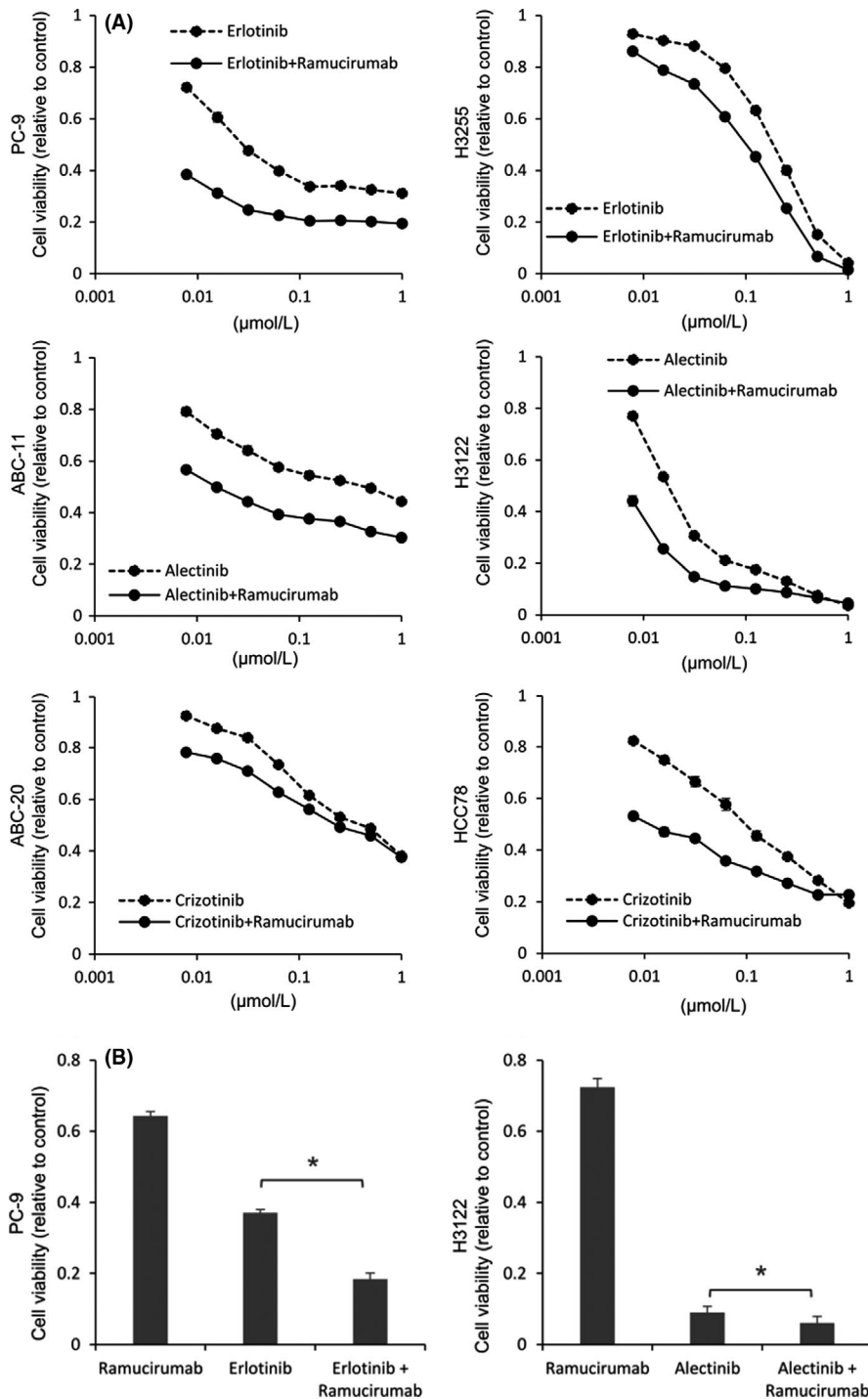
3.3 | VEGFR2 blockade enhances the antiproliferative effects of molecular targeted therapies in vitro

To determine whether VEGFR2 inhibition has any impact on oncogene-driven NSCLC cells themselves in addition to inhibiting tumor angiogenesis, we investigated the effects of VEGFR2 blockade in different NSCLC cell lines in vitro. As all of the cell lines used were derived from human NSCLC, we used the human anti-VEGFR2 antibody ramucirumab. We performed cell proliferation assays in *EGFR*-mutant (PC-9, H3255), *ALK*-rearranged (ABC-11, H3122), and *ROS-1*-rearranged (ABC-20, HCC78) NSCLC cells treated with erlotinib, alectinib, and crizotinib, respectively (Figure 3A,B). Although the difference was moderate, combination with ramucirumab significantly enhanced their antiproliferative effects in vitro, implying a potential role of VEGFR2 signaling in NSCLC cell proliferation. We also assessed the effects of
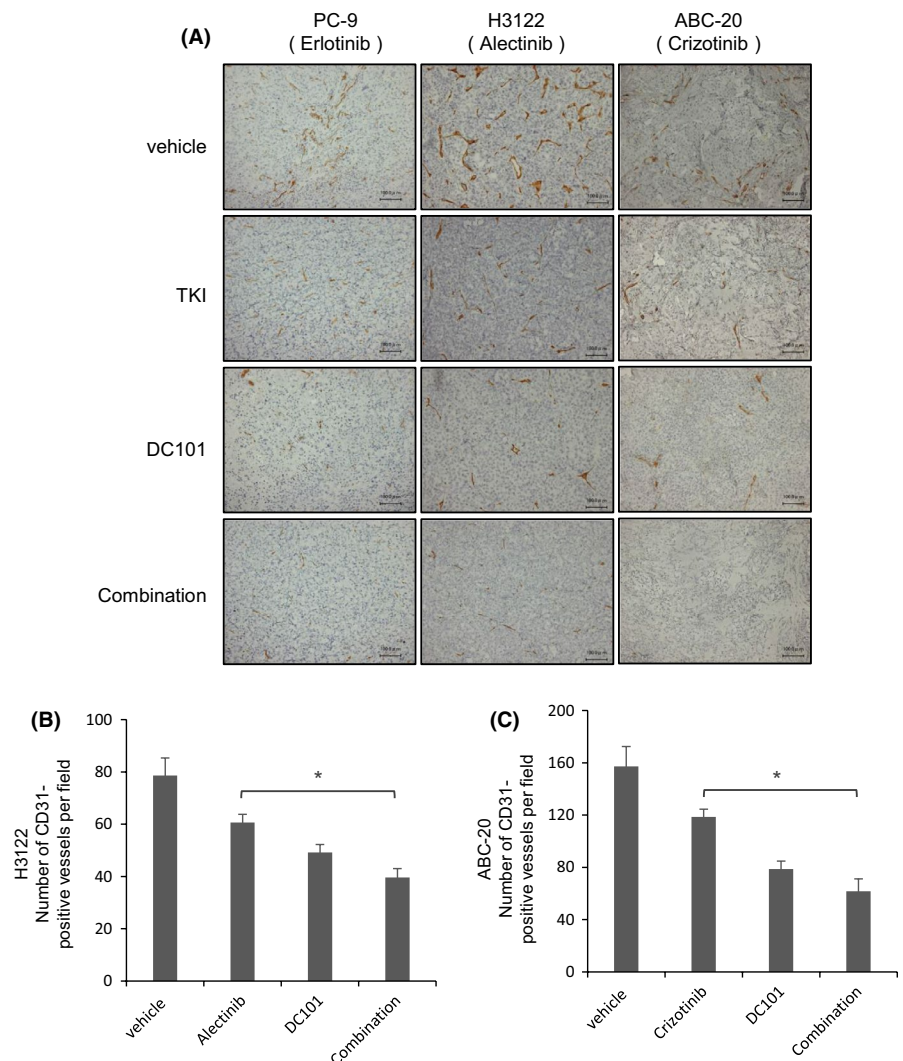
FIGURE 2 VEGFR2 blockade suppresses angiogenesis in xenograft mouse models. A, Immunohistochemical staining of CD31 in PC-9, H3122, and ABC-20 xenograft tumors. Scale bars: 100 μm. B, C, Number of CD31-positive blood vessels in tumors treated with the indicated drugs. Each bar indicates the average number of CD31-positive blood vessels in 5 fields. Error bars represent standard errors; *P < .005

FIGURE 3 VEGFR2 blockade enhances the antiproliferative effects of molecular targeted therapies in vitro. A, Cell proliferation assays in cells treated with the indicated concentrations of each molecular targeted agent. Ramucirumab was used at 150 μg/mL. All experiments were performed in triplicate, and representative data are shown. B, Antiproliferative effects of the combination therapy with erlotinib (100 nmol/L), alectinib (100 nmol/L), and ramucirumab (150 μg/mL) in PC-9 and H3122 cells over 96 h, as determined by MTT assay. Data are presented as means ± SE. *$P < .001$
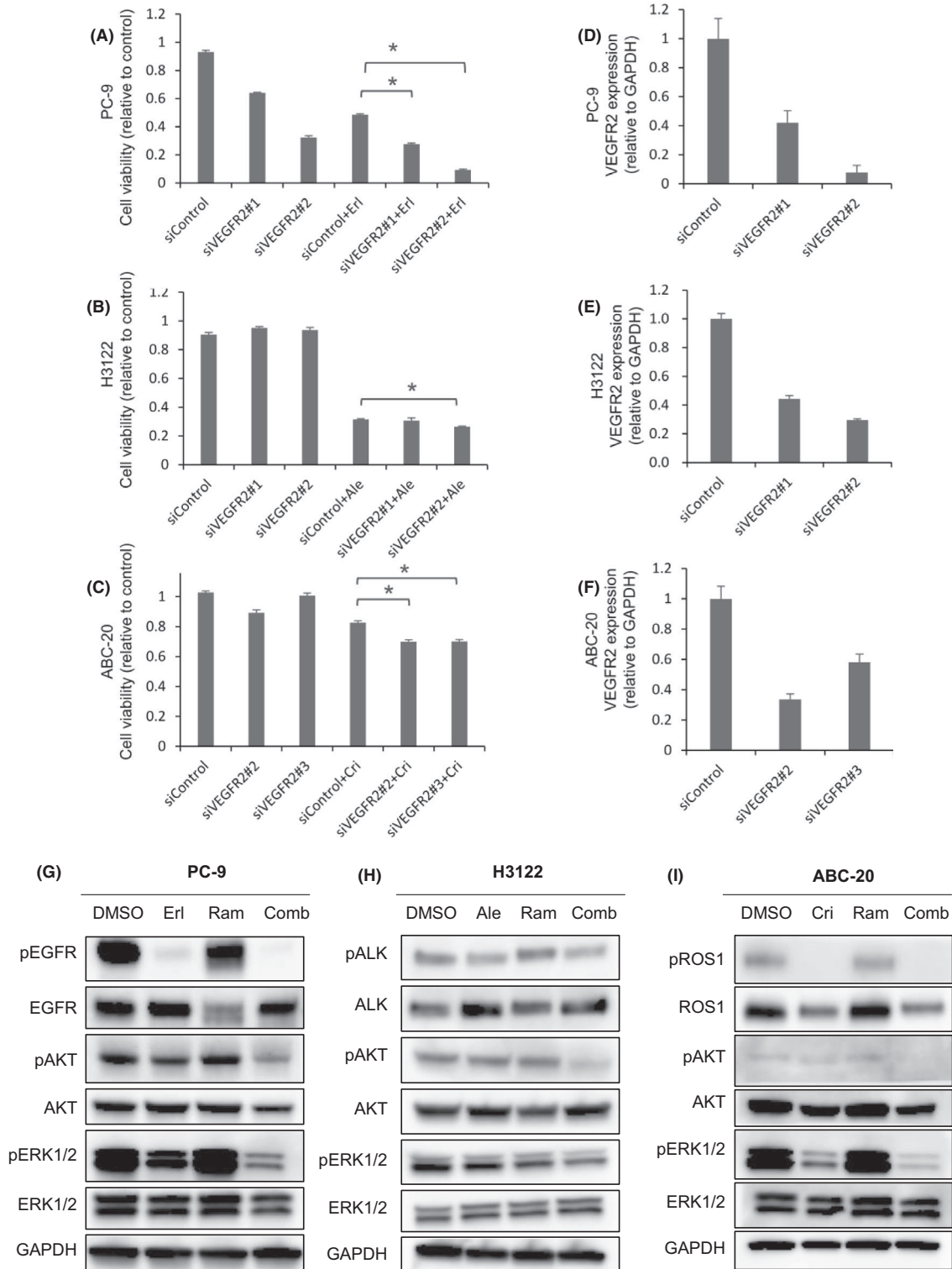
siRNA-mediated *VEGFR2* silencing combined with molecular targeted agents (Figure 4). Consistently, *VEGFR2* silencing significantly enhanced the antiproliferative effects of molecular targeted agents in PC-9, H3122, and ABC-20 cells (Figure 4A-C). Decreased VEGFR2 expression by siVEGFR2 was confirmed in all of these cells (Figure 4D-F).

We then investigated the effects of VEGFR2 inhibition on downstream signaling pathways. We found that cells treated with the combination therapies had lower phospho-ERK1/2 and phospho-AKT levels than did cells treated with molecular targeted agents alone in PC-9, H3122, and ABC-20 cells (Figure 4G-I). These findings imply that VEGFR2 signaling is involved in upstream AKT and ERK

pathways in oncogene-driven NSCLC, and that anti-VEGFR2 therapy, in addition to exerting antiangiogenic effects, could provide strong cell-intrinsic anti-tumor effects by interfering with various oncogenic pathways.

3.4 | VEGF-A and VEGFR2 are highly expressed in oncogene-driven NSCLC cells

To investigate the relationship between oncogenic pathways and VEGFR2 activation, we assessed the level of VEGF-A, a VEGFR2

FIGURE 4 Effects of *VEGFR2* silencing combined with molecular targeted agents on oncogenic signaling pathways and cell growth. A-C, Two different *VEGFR2*-targeting siRNAs were used. The effects of *VEGFR2* silencing on cell growth in PC-9, H3122, and ABC-20 cells. PC-9 cells were treated with erlotinib (100 nmol/L) for 96 h, H3122 cells with alectinib (100 nmol/L) for 96 h, and ABC-20 cells with crizotinib (1 μmol/L) for 96 h. All cell lines were treated with ramucirumab (150 μg/mL) for 96 h. *P < .005. D-F, qRT-PCR analysis showing efficient siRNA-mediated *VEGFR2* knockdown in different cell lines. *GAPDH* was used as the reference gene. Data are presented as means ± SE. G-I, Phospho-ERK1/2 (PC-9 and ABC-20 cells) and phospho-AKT levels (H3122 cells) were lower in cells treated with the combination therapy compared with in cells treated with the molecular targeted agents alone. PC-9, H3122, and ABC-20 cells were treated with erlotinib (100 nmol/L), alectinib (100 nmol/L), and crizotinib (1 μmol/L), respectively. All cell lines were also exposed to ramucirumab (150 μg/mL); all treatments were performed for 96 h
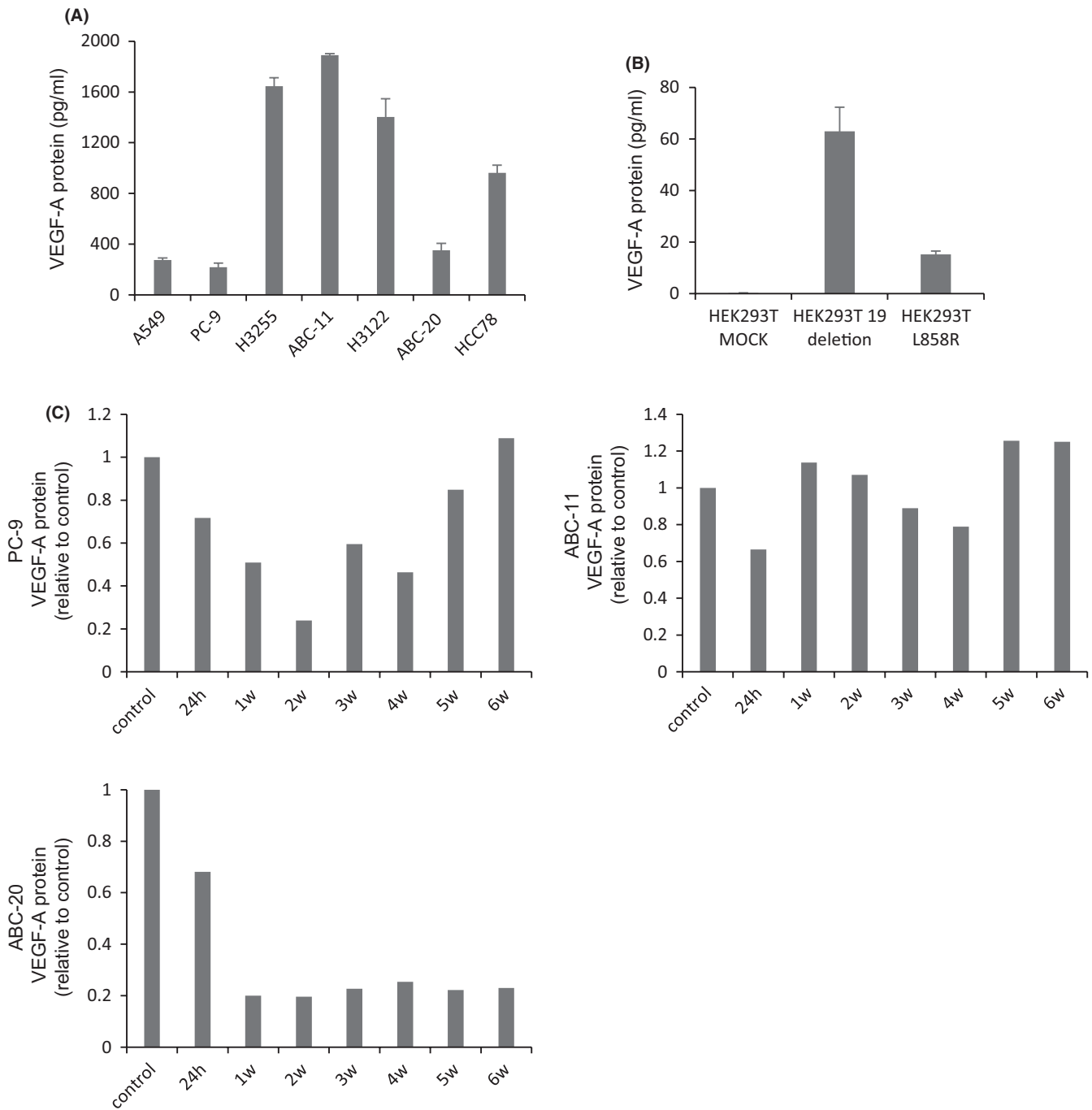
FIGURE 5 VEGF-A is highly expressed in oncogene-driven NSCLC cells. Cells were seeded into 3.5 cm dishes at 3.0×10^5 cells/2.0 mL, and the cell culture supernatant was collected after 24 h. A, The cell supernatant of *EGFR*-, *ALK*-, or *ROS1*-altered cell lines (H3255, ABC-11, H3122, HCC78, and ABC-20) contained higher VEGF-A levels compared with that of A549 control cells. B, HEK293T cells transfected with mutant *EGFR* (L858R or exon 19 deletion) exhibited higher levels of VEGF-A secretion compared with control cells. C, VEGF-A secretion after treatment with molecular targeted agents. PC-9, ABC-11, and ABC-20 cells were treated with erlotinib (100 nmol/L), alectinib (100 nmol/L), or crizotinib (100 nmol/L), respectively. Data are presented as means ± SE

ligand, in the cell culture supernatant of oncogene-driven NSCLC cells. A549 and H2009 cells, both of which are wild-type for *EGFR*, *ALK*, and *ROS-1*, were used as controls. The majority of cell lines harboring *EGFR*, *ALK*, or *ROS1* alteration exhibited higher VEGF-A protein levels compared with control A549 cells (Figure 5A). We also found that HEK293T cells expressing mutant *EGFR* (L858R or exon 19 deletion) had significantly higher VEGF-A protein levels

in the cell supernatant compared with control cells (Figure 5B), implying that VEGF-A secretion was driven by oncogenic signaling. Notably, treatment with erlotinib, alectinib, or crizotinib significantly decreased VEGF-A secretion (Figure 5C), confirming that VEGF-A production was driven by oncogenic signaling. Of note, long-term exposure to molecular targeted agents further increased VEGF-A secretion, indicating that VEGF-A would be

more important under long-term inhibition of oncogene signal inhibition. A cell proliferation assay at the time of VEGF-A recovery (after 6 wk of treatment) revealed early emergence of cellular acquired resistance, suggesting that VEGF-A recovery occurred after such resistance developed (Figure S3).

We also assessed *VEGFR2* expression at the mRNA level using qRT-PCR *VEGFR2* mRNA levels were significantly higher in *EGFR*-, *ALK*-, or *ROS1*-altered cells (PC-9, H3255, ABC-11, H3122, HCC78, and ABC-20) compared with control cells (A549 and H2009; Figure 6A). We next investigated the VEGFR2 expression levels in clinical samples of *EGFR*-mutant NSCLCs. VEGFR2 was expressed in 3 out of 4 lung cancers with *EGFR* mutations, although no expression was found in the 2 *EGFR/ALK/ROS1* wild-type NSCLCs (Figure 6B). Those data imply a potential role for VEGFR2 signaling in EGFR/ALK/ROS1-driven NSCLC. Of note, treatment with erlotinib, alectinib, or crizotinib significantly increased the *VEGFR2* mRNA level in *EGFR*-(PC-9, H3255), *ALK*- (ABC-11, H3122), or *ROS1*-altered (ABC-20, HCC78) NSCLC cells, respectively (Figure 6C). These findings imply that VEGF-A/VEGFR2 signaling in oncogene-driven NSCLC might be more critical under oncogene signal inhibition. Finally, we determined the VEGFR2 expression levels of the HEK293T model with or without mutant EGFR transfection (Figure S4). Unexpectedly, 19del or L858R transfection decreased VEGFR2 expression in HEK293T cells. Although the precise reason for this discrepancy from the data shown in Figure 6A,B remains unclear, forced expression may not simulate accurately the condition of *EGFR*-mutant lung cancer cells.

3.5 | VEGFR2 blockade augments the anti-tumor effects of TKIs by acting on both tumor cells and tumor vessels

In the human body, anti-human VEGFR2 therapy works on both cancer cells and micro-environmental tumor vessels. However, in our xenograft mouse model, the anti-human VEGFR2 antibody ramucirumab acted only on xenograft tumors, while the anti-mouse VEGFR2 antibody DC101 acted only on the vessels. Hence, to target VEGFR2 on both cancer cells and tumor vessels, we treated PC-9 xenograft tumors with both ramucirumab and DC101. We found that the combination of erlotinib, DC101, and ramucirumab provided the most potent anti-tumor effects in the xenograft mouse model (Figure 7A), with no significant toxicity (Figure 7B). Importantly, CD31 immunostaining revealed that the combination of DC101 and erlotinib or the triplet combination of DC101, ramucirumab, and erlotinib strongly inhibited vessels in the tumors treated (Figure 7C,D).

4 | DISCUSSION

In this study, we demonstrated that VEGFR2 blockade augmented the anti-tumor effects of molecular targeted agents in various oncogene-driven NSCLCs harboring *EGFR*, *ALK*, or *ROS1* alterations.

The enhanced anti-tumor effects of the combination therapy were mediated via direct inhibition of cancer cell growth, as well as antiangiogenic effects. We previously showed that bevacizumab, an anti-VEGF-A antibody, enhanced the effects of EGFR TKIs in *EGFR*-mutant NSCLC.[14-16] However, the effects of VEGFR2 blockade on the efficacy of EGFR TKIs or other molecular targeted agents in NSCLC were unclear. Therefore, in this study, we expanded our findings on the combination of anti-VEGF-A therapy with EGFR TKIs to VEGFR2 blockade combined with various molecular targeted agents in oncogene-driven NSCLC. We demonstrated that the anti-mouse VEGFR2 antibody DC101 enhanced the anti-tumor effects of molecular targeted agents in mice bearing *ALK*-, *ROS1*-, or *EGFR*-altered NSCLC.

Although the synergistic effects of anti-VEGF-A or anti-VEGFR2 antibodies with EGFR TKIs have been demonstrated in multiple clinical and preclinical studies,[10,11,14-16] the precise underlying mechanisms are unclear. In this study, we performed CD31 immunostaining and showed that the combination of molecular targeted agents and VEGFR2 blockade with DC101 profoundly inhibited tumor angiogenesis. As DC101 can act on mouse vessels but not on implanted human cancer cells, the enhanced anti-tumor effects of the combination therapy in the xenograft mouse models were attributed to the antiangiogenic effects of VEGFR2 blockade.

In contrast with the well established roles of VEGFR2 signaling in angiogenesis, the cell-intrinsic effects of anti-VEGFR2 therapy on cancer cells are less clear. Cancer cells express VEGFRs, and autocrine VEGF/VEGFR signaling promotes cancer cell growth, survival, migration, and invasion.[17] However, the relevance of VEGFR signaling in oncogene-driven NSCLC was unknown. To determine the cell-intrinsic effects of anti-VEGFR2 therapy on oncogene-driven NSCLC cells, we treated different human NSCLC cell lines with an anti-human VEGFR2 antibody, ramucirumab, in vitro. The combination of ramucirumab with molecular targeted agents potentiated the antiproliferative effects of these agents, implying a cell-intrinsic role of VEGFR2 signaling in oncogene-driven NSCLC.

VEGF-A expression is induced by various factors, including EGFR[18], however a possible association between VEGFR signaling and ALK, or ROS-1 signaling, in lung cancer remains elusive. In this study, we demonstrated that oncogenic signaling pathways influenced the expression of VEGF-A and VEGFR2; VEGF-A was highly expressed in *EGFR/ALK/ROS1*-driven NSCLC cells (Figure 5A) and was induced by forced overexpression of mutant *EGFR* (Figure 5B). These data highlighted the fact that oncogenic signaling pathways can induce VEGFR2 pathway activation. Of note, the *VEGFR2* mRNA levels were also elevated in *EGFR/ALK/ROS1*-driven NSCLC cells (Figure 6A) and were further increased after treatment with molecular targeted agents (Figure 6C), whereas the VEGF-A levels decreased transiently after treatment (Figure 5C). These data implied that the VEGFR2 signaling axis plays an important role in oncogene-driven lung cancers; VEGFR2 levels would increase as a complemental response to the transient decrease in VEGF-A levels induced by inhibition of oncogene signaling.

Another research group has investigated the therapeutic effects of a similar treatment strategy on oncogene-driven cancer. In their
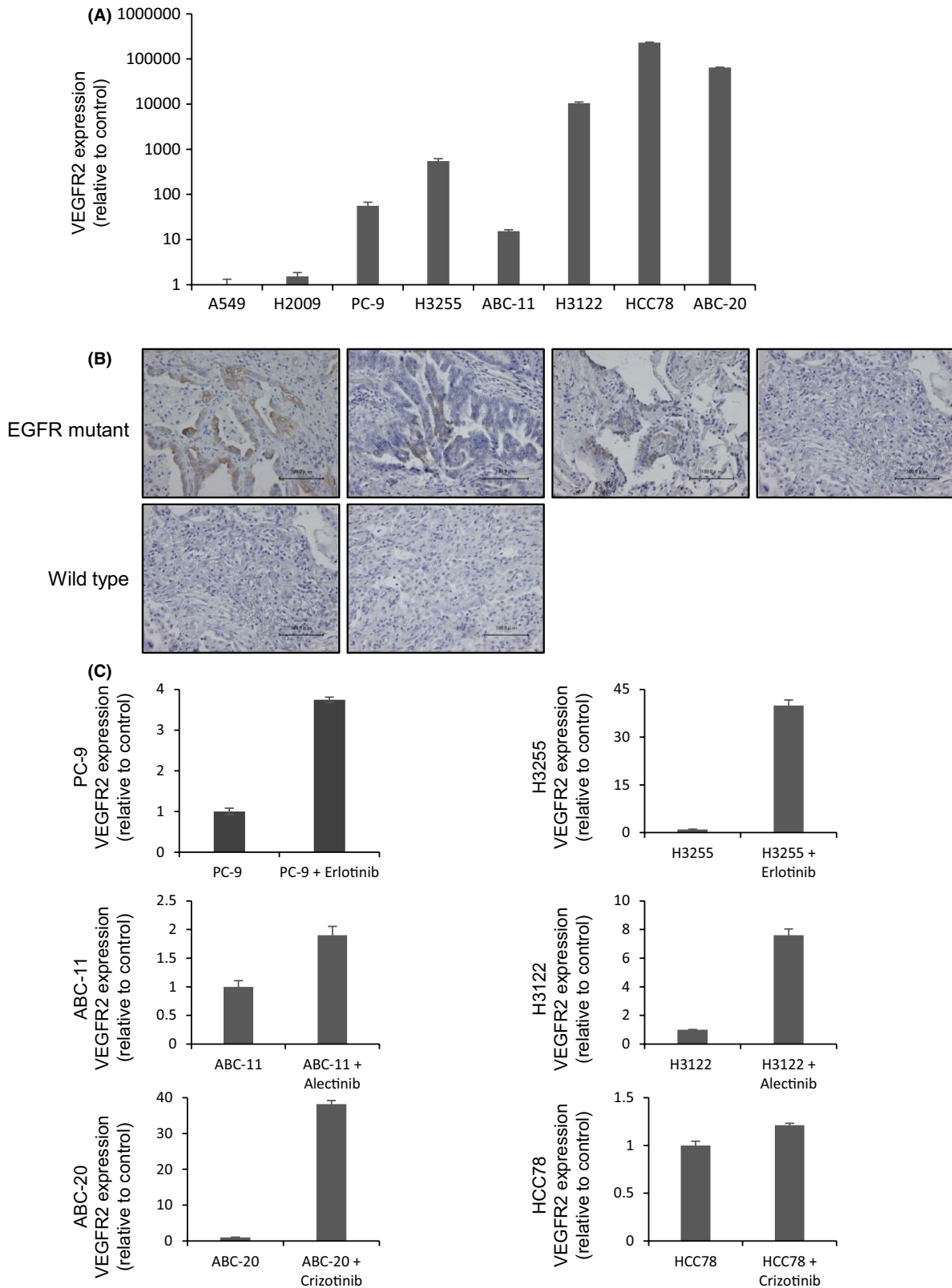
FIGURE 6 VEGFR2 is highly expressed in oncogene-driven NSCLC cells. A, qRT-PCR of *VEGFR2* in PC-9, H3255, ABC-11, H3122, HCC78, and ABC-20 cells. *GAPDH* was used as the reference gene. Data are presented as means ± standard error. B, Clinical specimens of tumors bearing EGFR mutations exhibited higher levels of VEGFR2 expression than did EGFR-wild-type tissues, as revealed by immunostaining. C, Increased *VEGFR2* expression induced by treatment with erlotinib, alectinib, or crizotinib in accordance with qRT-PCR. PC-9, ABC-11, and ABC-20 cells were treated with erlotinib (100 nmol/L), alectinib (100 nmol/L), or crizotinib (1 μmol/L), respectively, for 24 h. Data are presented as means ± SE

study, they inhibited oncogenic drivers in combination with targeting the VEGF co-receptor neuropilin-1.[19,20] This combination therapy exerted potent anti-tumor effects in vitro in oncogene-driven melanoma and breast cancer cells,[21] further supporting our findings regarding the importance of VEGFR2 as a therapeutic target in combination with molecular targeted agents.

In conclusion, we found that VEGFR2 blockade augmented the anti-tumor effects of molecular targeted agents in oncogene-driven NSCLC, particularly in *EGFR/ALK/ROS1*-driven NSCLC. We also identified two mechanisms underlying the synergistic effects of anti-VEGFR2 therapy with molecular targeted agents. VEGFR2 blockade not only inhibited tumor angiogenesis but also exerted direct antiproliferative effects on
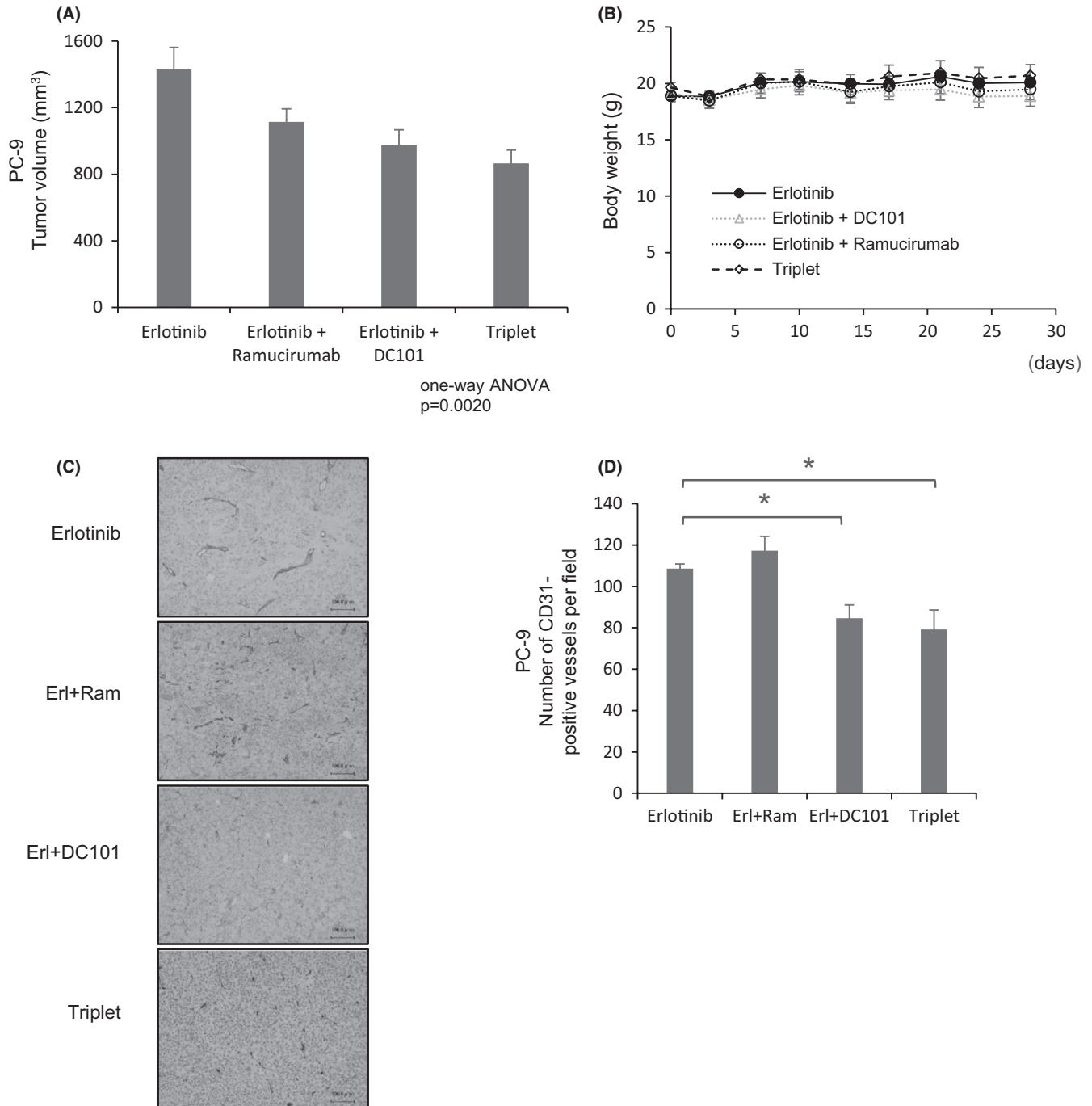
FIGURE 7 VEGFR2 blockade augments the anti-tumor effects of TKIs in mice bearing PC-9 tumors. A, Mice bearing PC-9 tumors were treated with erlotinib, erlotinib plus DC101, erlotinib plus ramucirumab, or triplet therapy. Erlotinib (30 mg/kg/d) was administered intraperitoneally 5 times weekly. DC101 and ramucirumab (10 mg/kg/d) were administered intraperitoneally twice weekly. B, Body weight of mice bearing PC-9 tumors. C, Immunohistochemical staining of CD31 in mice bearing PC-9 tumors. Scale bars: 100 μm. D, Number of CD31-positive blood vessels in tumors treated with the indicated drugs. Each bar indicates the average number of CD31-positive blood vessels in 5 fields. Error bars represent standard errors; *$P < .05$

cancer cells. Thus, combination therapy with ramucirumab and molecular targeted agents could serve as a promising treatment strategy for *ALK-* or *ROS1*-rearranged NSCLC, in addition to *EGFR*-mutant NSCLC.

ORCID

Eiki Ichihara https://orcid.org/0000-0002-2966-106X
Go Makimoto https://orcid.org/0000-0002-0638-8435
Hirohisa Kano https://orcid.org/0000-0003-4327-7547
Kadoaki Ohashi https://orcid.org/0000-0002-5180-3933

REFERENCES

1. Paez JG, Jänne PA, Lee JC, et al. EGFR mutations in lung cancer: Correlation with clinical response to gefitinib therapy. *Science.* 2004;304:1497-1500.
2. Soda M, Choi YL, Enomoto M, et al. Identification of the transforming EML4-ALK fusion gene in non-small-cell lung cancer. *Nature.* 2007;448:561-566.
3. Takeuchi K, Soda M, Togashi Y, et al. RET, ROS1 and ALK fusions in lung cancer. *Nat Med.* 2012;18:378-381.
4. Rikova K, Guo A, Zeng Q, et al. Global Survey of phosphotyrosine signaling identifies oncogenic kinases in lung cancer. *Cell.* 2007;131:1190-1203.
5. Maemondo M, Inoue A, Kobayashi K, et al. Gefitinib or chemotherapy for non-small-cell lung cancer with mutated EGFR. *N Engl J Med.* 2010;362:2380-2388.
6. Solomon BJ, Mok T, Kim DW, et al. First-line crizotinib versus chemotherapy in ALK-positive lung cancer. *N Engl J Med.* 2014;371:2167-2177.
7. Shaw AT, Ou SH, Bang YJ, et al. Crizotinib in ROS1-rearranged non-small-cell lung cancer. *N Engl J Med.* 2014;371:1963-1971.
8. Viallard C, Larrivée B. Tumor angiogenesis and vascular normalization: alternative therapeutic targets. *Angiogenesis.* 2017;20:409-426.
9. Sandler A, Gray R, Perry MC, et al. Paclitaxel-carboplatin alone or with bevacizumab for non-small-cell lung cancer. *N Engl J Med.* 2006;355:2542-2550.
10. Saito H, Fukuhara T, Furuya N, et al. Erlotinib plus bevacizumab versus erlotinib alone in patients with EGFR-positive advanced non-squamous non-small-cell lung cancer (NEJ026): interim analysis of an open-label, randomised, multicentre, phase 3 trial. *Lancet Oncol.* 2019;20:625-635.
11. Nakagawa K, Garon EB, Seto T, et al. Ramucirumab plus erlotinib in patients with untreated, EGFR-mutated, advanced non-small-cell lung cancer (RELAY): a randomised, double-blind, placebo-controlled, phase 3 trial. *Lancet Oncol.* 2019;2045:1-15.
12. Isozaki H, Yasugi M, Takigawa N, et al. A new human lung adenocarcinoma cell line harboring the EML4-ALK fusion gene. *Jpn J Clin Oncol.* 2014;44:963-968.
13. Kato Y, Ninomiya K, Ohashi K, et al. Combined effect of cabozantinib and gefitinib in crizotinib – resistant lung tumors harboring *ROS1* fusions. *Cancer Sci.* 2018;109(10):3149-3158.
14. Ichihara E, Ohashi K, Takigawa N, et al. Effects of vandetanib on lung adenocarcinoma cells harboring epidermal growth factor receptor T790M mutation in vivo. *Cancer Res.* 2009;69:5091-5098.
15. Ninomiya T, Takigawa N, Ichihara E, et al. Afatinib prolongs survival compared with gefitinib in an epidermal growth factor receptor-driven lung cancer model. *Mol Cancer Ther.* 2013;12:589-597.
16. Ichihara E, Hotta K, Nogami N, et al. Phase II trial of gefitinib in combination with bevacizumab as first-line therapy for advanced non-small-cell lung cancer with activating EGFR gene mutations: The Okayama Lung Cancer Study Group trial 1001. J Thorac Oncol. International Association for the Study of. *Lung Cancer.* 2015;10:486-491.
17. Goel HL, Mercurio AM. VEGF targets the tumour cell. *Nat Rev Cancer.* 2013;13:871-882.
18. Tabernero J. The role of VEGF and EGFR inhibition: Implications for combining anti-VEGF and anti-EGFR agents. *Mol Cancer Res.* 2007;5:203-220.
19. Amadio M, Govoni S, Pascale A. Targeting VEGF in eye neovascularization: What's new?: A comprehensive review on current therapies and oligonucleotide-based interventions under development. *Pharmacol Res.* 2016;103:253-269.
20. Jarvis A, Allerston CK, Jia H, et al. Small molecule inhibitors of the neuropilin-1 vascular endothelial growth factor A (VEGF-A) interaction. *J Med Chem.* 2010;53:2215-2226.
21. Rizzolio S, Cagnoni G, Battistini C, et al. Neuropilin-1 upregulation elicits adaptive resistance to oncogene-targeted therapies. *J Clin Invest.* 2018;128:3976-3990.

SUPPORTING INFORMATION

Additional supporting information may be found online in the Supporting Information section.